

Article

Deep learning and hand-crafted features for virus image classification

Loris Nanni ¹, Eugenio De Luca ¹ and Marco Ludovico Facin ^{1,*}

¹ DEI. Via Gradenigo 6, 35131 Padova, Italy; loris.nanni@dei.unipd.it (L.N.); eugenio.deluca@studenti.unipd.it (E.D.L.); marcoludovico.facin@studenti.unipd.it (M.L.F.)

* Correspondence: loris.nanni@unipd.it

Received: date; Accepted: date; Published: date

Abstract: In this work, we present an ensemble of descriptors for the classification of transmission electron microscopy images of viruses. We propose to combine handcrafted and deep learning approaches for virus image classification. The set of handcrafted is mainly based on Local Binary Pattern variants, for each descriptor a different Support Vector Machine is trained, then the set of classifiers is combined by sum rule. The deep learning approach is a densenet201 pretrained on ImageNet and then tuned in the virus dataset, the net is used as features extractor for feeding another Support Vector Machine, in particular the last average pooling layer is used as feature extractor. Finally, classifiers trained on handcrafted features and classifier trained on deep learning features are combined by sum rule. The proposed fusion strongly boosts the performance obtained by each stand-alone approach, obtaining state of the art performance. The MATLAB code of the proposed ensemble is available at <https://github.com/LorisNanni>.

Keywords: virus classification; texture descriptors; deep learning; local binary patterns; ensemble of descriptors.

1. Introduction

Recognising and classifying viruses is fundamental to the medical field for both diagnosis and research. Since it's so important and since it requires highly qualified medical-staff to be done, it brought to itself more and more attention over the years.

One of the first applications of computer vision aimed at the study of viruses is described in [1] published in 2002 in which ring filters are used on a dataset of images of four classes of viruses for the extraction of features; in the same abstract of the paper is said “To reduce the diagnosis time and to de-skill the diagnosis task by allowing the use of non-specialist medical staff, an automatic virus recognition method is presented.” evidences that not enough research had yet been done in the field of automation applied to the classification of viruses and it was therefore necessary to rely on highly qualified personnel to carry it out.

The method proposed in [1] uses a Bayesian classifier with an overall accuracy of 98% in the worst case.

Nine years later, in 2011, in [2] it has been tried to use the features extracted from LBP and LDP on the same dataset treated in this study using a Random Forest classifier; the results show that the average error obtained overall is 13%.

Moreover in 2013 Maria C. Proen  a et alia's paper [3] proposed a feature extracting method for polyomavirus images to automate its segmentation process.

In 2015, innovative feature descriptors (and their merger) were tested in [4] to improve the performance of the FUSION ensemble described in [5], effectively achieving better performance by 5%.

The following year, in [6], the combination of multi-PCA and multi-CLBP with an overall accuracy of 86.20% is proposed by Zhijie Wen on the same dataset treated in this study.

More recent studies propose the application of transfer learning on pre-trained Convolutional Neural Networks (SqueezeNet, DenseNet, ResNet and InceptionV3) [7] on the same dataset used on our paper.

In 2020, in [8], is proposed by André R. Backes et al a study aimed at the application of various extractors on our same dataset (such as Gabor Wavelets, Randomized Neural Network signature and others) with promising results: the combination of all these methods led to an average accuracy of 87.27%.

In the same year Zhi-Jie Wen et al applied on the same dataset a method based on the use of images filtered through Principal Component Analysis and Gaussian filters obtaining an overall accuracy of 88%, the highest ever obtained on that dataset until then [9].

In summary, the application of AI in the field of virus classification and in medicine in general is still evolving with increasing performance: these techniques as well as becoming increasingly reliable can replace highly skilled personnel in these particularly tedious tasks.

In this work, we expand previous works on ensemble of descriptors for virus classification combining both handcrafted features and deep learning.

A large set of handcrafted features is used for training a set of Support Vector Machines (SVM) then combined by sum rule; another SVM is trained using the features extracted by the last average pooling layer of a DenseNet201 neural networks pre-trained on ImageNet and then tuned on the virus images.

The experimental results confirm the validity of the proposed method, our proposed ensemble obtains state of the art performance in the tested dataset, the MATLAB code used in this study will be available at <https://github.com/LorisNanni>.

The present paper is organized as follows. In [Section 2](#) different information on Viruses are detailed. In [Section 3](#) we describe the different approaches used to feed Support Vector Machine (SVM) classifiers. In [Section 4](#) the experimental results are reported and some conclusions are drawn.

2. Materials

2.1 What is a Virus?

A virus is a sub microscopic agent who's able to replicate inside a living organism's cell only. As we see in [10] we only have a detailed description of 6590 virus species, however as stated in [11] 10^{31} are the species estimated to exist on planet Earth; for example more than 5000 different virus genotypes can be found in only 200 litres of seawater.

Seeing these numbers it becomes clear how much virus research, and consequently their classification, is important nowadays.

Viruses can have very different shape and size between species, but they are in general composed of a nucleic acid and a protective protein membrane that wraps it called capsid; this whole particle is called virion. Morphologically 5 kinds of viruses are known ([Figure 1](#)):

Icosahedral: They have an icosahedral shape, sometimes very similar to a sphere.

Prolate: they have a lengthened icosahedral shape, it's common for bacteriophage viruses.

Helical: the helicoidal shape can present an empty cavity inside; viruses with this shape can be short and rigid, or long and flexible.

Involucro: Some viruses wrap themselves in a cellular membrane and it can be the external membrane or the internal one (like the nuclear membrane) of the attacked cell. This membrane is known as "viral envelope".

Complex: they are particular viruses the capsid of which is neither totally helicoidal nor icosahedral and it can have unusual structures like proteic tails.

2.2 Viruses and humans

Viruses relate with the hosting organism differently from one another, so it's hard to define a common behaviour.

For example, as stated in [12], there are viruses that only infect insects (*Insect Specific Virus*) that cannot infect humans, while there are others, called Arboviruses, that can pass from insects to humans: for example a very known one from this category is the Yellow Fever.

However, as stated in [13], the pathogenesis, how a disease is born and/or it develops, has common phases that differ from each other by small details but they have the same goal.

The pathogen penetrates the human organism and infects some cells where it begins its replication process that varies based on its genome (RNA, DNA) [14].

After this first infection stage the sentinel cells activate themselves to amplify the immune response that will adapt over time to thoroughly eliminate the pathogen from the organism.

When the virus is eradicated some cells called B and T are responsible for storing the antigen that caused the infection: in this way if the antigen should ever recur in our body these specialized units will respond to the infection instantly.

This ability of our immune system is called immunological memory which, despite protecting us every day from the many pathogens with which we come into contact, is unfortunately not an infallible weapon: the mutation of the virus itself, for example, can evade our immunological memory by allowing it to infect us again.

This problem occurs every year with seasonal influenza and there are numerous studies such as [15] which propose methods to strengthen annual influenza vaccines which, at the historical moment in which this document is written, protect only for one year.

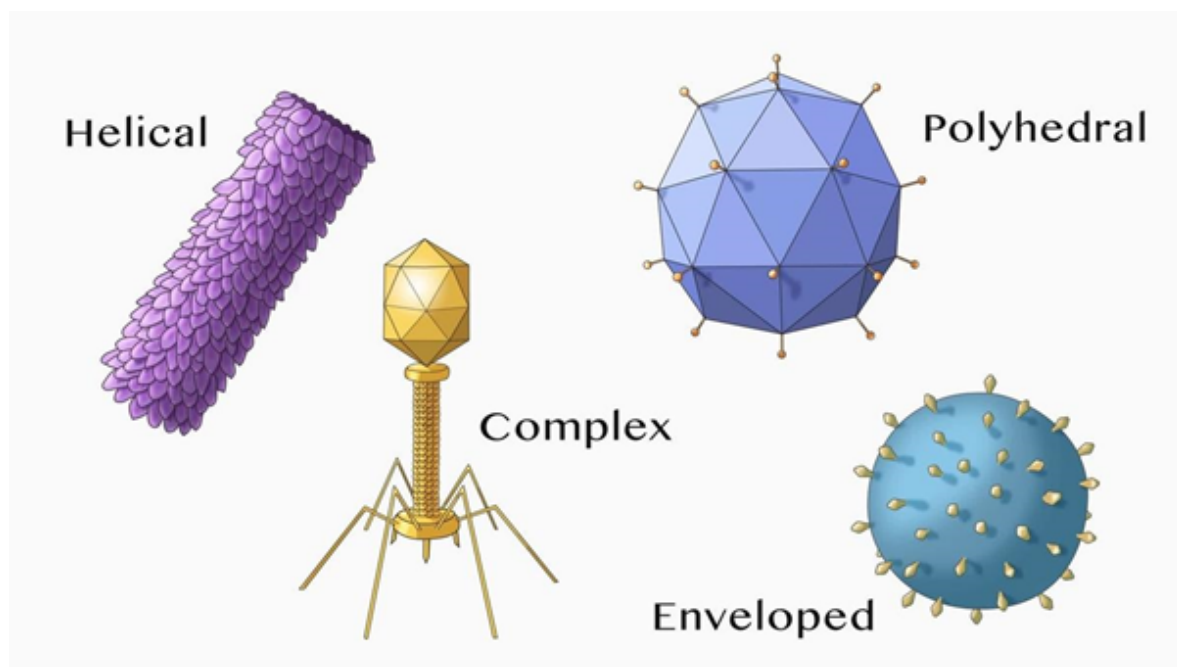


Figure 1. Various virus shapes

2.3 Reasons behind virus classification

During 1966 the International Committee on Nomenclature of Viruses (ICNV) was founded in Moscow during the National Microbiology Congress with the aim of building a solid taxonomic system for the classification of viruses; its name was changed in 1974 to “International Committee on Taxonomy of Viruses (ICTV)”.

However, it is only in 1995 that the ICTV will adopt a uniform and solid taxonomic system for the classification of viruses: its name is *Universal Virus Classification* and includes 3 orders, 73 families, 9 subfamilies, 287 genera and 5450 viruses belonging to 1950 species [16].

However, where is the need for a comprehensive classification for viruses? Man by his nature tends to classify, organize, label what he does not know, however the need for a solid taxonomic system does not reside totally nor in the innate curiosity of the human being, nor the undeniable help this provides in medical diagnosis.

What is really important is that each category of virus possesses unique physicochemical particularities; consequently assigning a virus to a category means being able to know these characteristics a priori, that inevitably facilitate the choice of medical treatments useful to the case.

In short, a solid taxonomic system allows to abstract the peculiarities of each virus, facilitating its recognition and subsequent treatment.

2.4 Difficulties in virus classification

The main difficulty in classifying viruses is, very trivially, their large number: from 1993 to 2006, for example, the number of classified viruses has grown exponentially thanks to the DNA sequencing technique.

In addition to the large amount of existing viruses, however, there are other factors that make the creation of their accurate taxonomy complex: their replication and genetic heritage.

As stated in [17], in fact, each virus replicates in different ways depending on the biological situation in which it is found, making it extremely complex to categorize them only according to their behavior.

As for the genetic patrimony, viruses tend to exchange genetic material both with the host organism and among the like, making it very difficult to highlight what is "their nature": for each new virus discovered we do not know which organisms came into contact with, and therefore how much genetic material was exchanged.

Also, in [17] we learn that pairwise Analysis is used in the classification of viruses in which two viral genomes are selected randomly and it is calculated how many are the pairs of genes shared to evaluate their correlation.

In this way we generate a network, in which viruses are nodes and the various connections are built based on the genes shared between them, instead of a tree structure.

3. The Proposed Method

This section is divided into an introduction of SVM followed by the methods tested in this paper and those used in previous works, finally a description of Deep Learning approach. To avoid misunderstandings on parameter values, the code of each descriptor is available on <https://github.com/LorisNanni>.

3.1 Support Vector Machine

The name SVM stands for Support Vector Machines; describing them superficially, their goal is, given a dataset with two classes, to find the best hyperplane that separates them correctly and coherently (Nanni [33]).

Imagine then to have a set of data as in [Figure 3.1.1](#), the idea is to find a hyperplane (in this case it is a straight line since the data space has two dimensions) that separates the class "green" from "red".

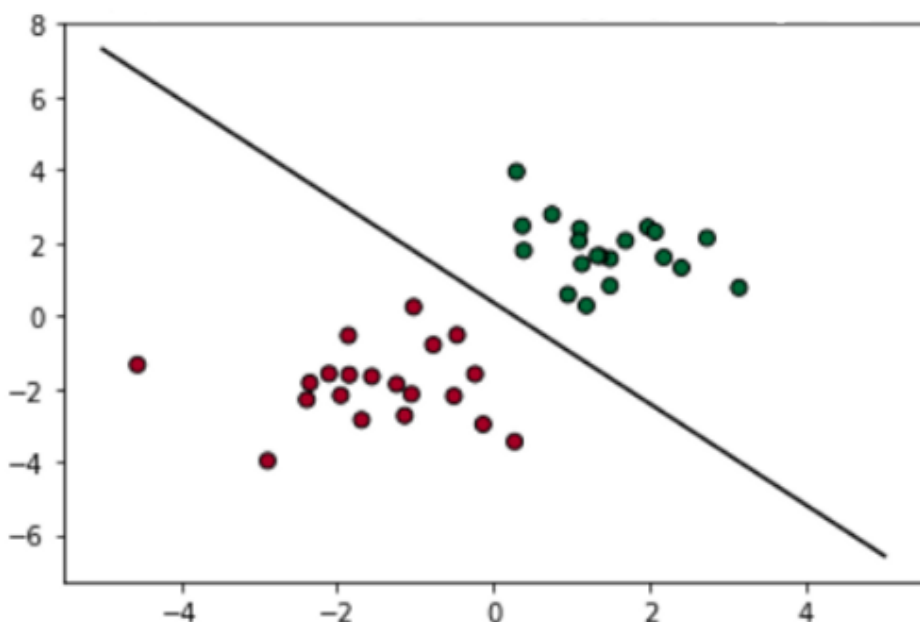


Figure 3.1.1. Simple bidimensional dataset with two classes

There are, however, infinite separation hyperplanes that divide the two classes, it is therefore necessary to evaluate what is the one that guarantees the greatest possible reliability. In order to carry out this type of assessment we must introduce the concept of margin, defined as follows:

$$\text{margin} = \min_{p \in P} (\text{distance}(\beta, p))$$

In other words, given a class, we define as a margin the minimum distance between all the points of the latter and the separation hyperplane, as shown in [Figure 3.1.2](#).

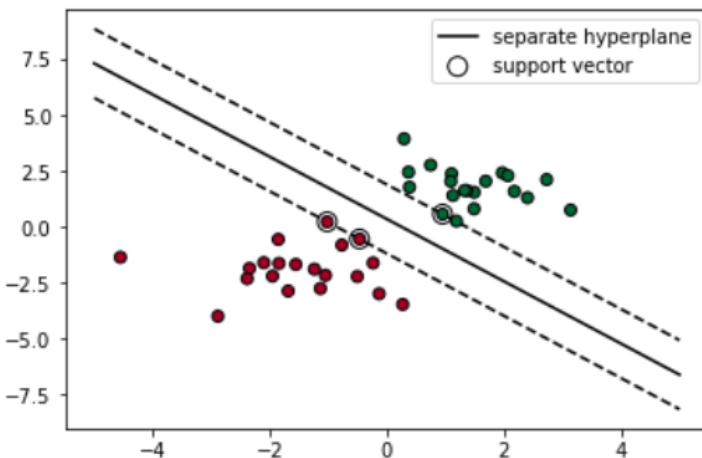


Figure 3.1.2. Separation hyperplane with its margin

The points lying on the margin are the most complex to classify and are called support vectors, their number characterize the difficulty of the classification problem.

When the spatial arrangement of the data does not allow to find a linear hyperplane that subdivides them coherently, one can choose the linear hyperplane that admits the least possible classification errors.

Otherwise you can do what is called Kernel Trick, that is the addition of new features that correspond to some combination of the existing ones depending on the kernel function used; increasing the dimensionality of the data can in fact make possible the existence of a linear hyperplane that divides them.

3.2 Texture descriptors Tested in this paper

3.2.1 Local Binary Pattern (LBP)

LBP operator provides a descriptor for any image using the gray levels of each pixel. In its classic version taken a pixel are considered the 8 adjacent to him thus creating a square of 3*3 pixels (Nanni [\[33\]](#)).

Then for each of these 8 neighbors their relationship with the central pixel is evaluated: if their grey level is greater than that of the central pixel they are replaced by a 1, otherwise by a 0.

The resulting binary pattern is then converted in a decimal number. The LBP operator is thus evaluated:

$$LBP(x_c, y_c) = \sum_{p \in P} 2^p \cdot q(i_p - i_c)$$

Where P is a structure that describes pixels close to the central one, i_c and i_p are respectively the grey levels of the central pixel and its p-th neighbor, and $q(z)$ is a quantization function defined as:

$$q(z) = \begin{cases} 1, & \text{if } z \geq 0 \\ 0, & \text{otherwise} \end{cases}$$

It's worth noticing that the number of neighbors and the radius are parameters that can be modified at will and are not static.

3.2.2 Discrete Local Binary Pattern (DLBP)

Described by Takumi Kobayashi [\[19\]](#) this algorithm is a modified version of Local Binary Pattern.

The idea is to find, for each pixel patch, the best threshold that divides the pixels inside it. This threshold is obtained by minimizing a residual error calculated as such:

$$\epsilon(\tau) = \frac{1}{N} \left\{ \sum_{i|I(r_i) \leq \tau} (I(r_i) - \mu_0)^2 + \sum_{i|I(r_i) > \tau} (I(r_i) - \mu_1)^2 \right\}$$

With:

$$\mu_0 = \frac{1}{N_0} \sum_{i|I(r_i) \leq \tau} I(r_i) \quad \text{and} \quad N_0 = \sum_i q(\tau - I(r_i))$$

$$\mu_1 = \frac{1}{N_1} \sum_{i|I(r_i) \geq \tau} I(r_i) \quad \text{and} \quad N_1 = \sum_i q(I(r_i) - \tau)$$

The residual error $\epsilon(\tau)$ is then configured as the intra-class variance σ_w^2 . The best threshold is the one that maximises the variance between classes σ_B^2 of the pixels in the patch calculated as such:

$$\sigma_B^2 = \sigma^2 - \sigma_w^2$$

Once this threshold is found the weight of each pixel patch on the final histogram is calculated:

$$\omega = \sqrt{\frac{\sigma_B^2(\gamma^*)}{\sigma^2 + C}}$$

Where C is a constant that serves to handle those cases where σ^2 is close to zero and may cause the weight of the vote to fluctuate too much. In Kobayashi's paper it is placed at 0.01². The feature is extracted with (radius,neighbors) = (1,8) , (2,8) , (3,8).

3.2.3 Sorted Consecutive Local Binary Pattern (scLBP)

The Sorted Consecutive Local Binary Pattern (scLBP) algorithm has been described by Jongbin Ryu et al during 2015 in [\[34\]](#).

This particular approach tries to solve some inconsistencies in the Rotation Invariant Local Binary Pattern. In scLBP from each pixel patch are extracted four components: SCLBP_S, SCLBP_M+, SCLBP_M-, SCLBP_C.

These components are then encoded by counting how much consecutive 0s and 1s there are and saving the result in two different array that will be sorted and concatenated.

For example, the pattern {00111010} will be encoded in {3, 1, 0} and {2, 1, 1} and then in {3, 1, 0, 2, 1, 1}. After this step the histogram is obtained through dictionary learning with kd-tree on the raw feature of each pixel of the image, however in our study we used k-means with 255 clusters instead of the kd-tree.

Centerpixel is a 16 element cell vector, each cell contains a matrix of centroids for each possible radius (for radius equal to 1 to 4 in steps of 0.2, so 16 elements).

3.2.4 Attractive Repulsive Center Symmetric Local Binary Pattern (ARCSLBP)

ARCSLBP is a LBP variant proposed by El merabet et al. [21], from a grey scale portion of image it considers four triplets around the center pixel (Figure 3.2.4.1 (a)) and Average Local Grey Level (ALGL), Average Global Grey Level (AGGL) and the mean value of the considered neighbors.

As can be seen in Figure 3.2.4.1 (b) the pattern of single ACSLBP is shorter than standard LBP and, more important, is different for the two portion of image considered, carrying more information than LBP which is the same. In a 8 neighbors case LBP method has a result histogram with 2^8 possible patterns, ACSLBP only 2^7 .

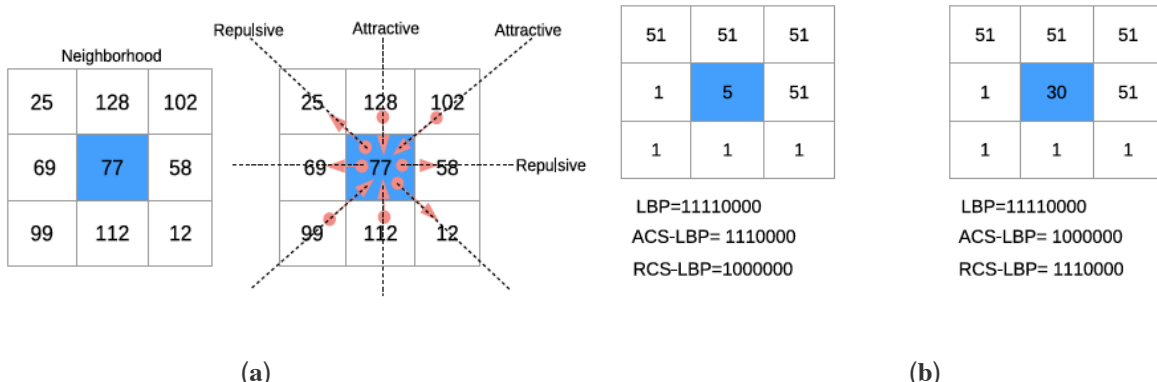


Figure 3.2.4.1. Representation of ARCSLBP: (a) Example of possible triplets center symmetric; (b) Example of various methods patterns.

The final ARCSLBP length is 2^8 (2^7 ACSLBP + 2^7 RCSLBP) which is the same of LBP but with improved performance as proved by El merabet et al. [21].

In this paper ARCSLBP is proposed with the variant of radius and neighbors, like standard LBP, the number of triplets can go up to half the neighbors (for example 8 triplets in 16 neighbors case), also Average Local Gray Level (ALGL) and average neighbors value are affected. The final histogram length is $2^{(\text{half of the neighbors} + 3)}$. The feature is extracted with (radius,neighbors) = (1,8) , (2,8) , (3,8).

3.2.5 Sigma Attractive Repulsive Center Symmetric Local Binary Pattern (sigmaARCSLBP)

Alpaslan et al. [21] merge the effectiveness of ARCSLBP with the Hessian matrix directional derivative information (Figure 3.2.5 (a)).

$$H(I(x, y)) = \begin{bmatrix} I_{xx} = \frac{d^2 I(x, y)}{dx^2} & I_{xy} = \frac{d^2 I(x, y)}{dxdy} \\ I_{yx} = \frac{d^2 I(x, y)}{dxdy} & I_{yy} = \frac{d^2 I(x, y)}{dy^2} \end{bmatrix}$$

$$G_{xx} = \frac{1}{2\pi\sigma^4} \left(\frac{x^2}{\sigma^2} - 1 \right) e^{-\frac{x^2+y^2}{2\sigma^2}} \quad G_{yy} = \frac{1}{2\pi\sigma^4} \left(\frac{y^2}{\sigma^2} - 1 \right) e^{-\frac{x^2+y^2}{2\sigma^2}}$$

(a)

$$I_{xx} = I * G_{xx} \quad I_{yy} = I * G_{yy} \quad Mag = \sqrt{I_{xx}^2 + I_{yy}^2}$$

(b)

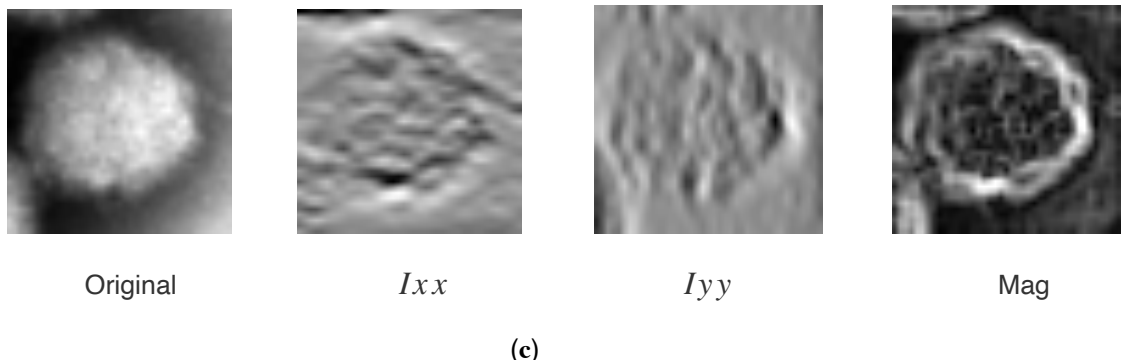


Figure 3.2.5. (a) Hessian Matrix Definition. (b) Second-order derivatives of Gaussian function and Magnitude definition with $\sigma(\sigma)$. (c) Example of Magnitude with Gaussian Standard Deviation $\sigma = 1$ (Lassa Virus).

The magnitude information of the Hessian matrix (Figure 3.2.5 (b)) with different σ variance values is used in the ACS-LBP method with variable radius and neighbors. The magnitude is useful to identify intense or flat portions of image (Figure 3.2.5 (c)). The feature is extracted with (radius,neighbors) = (1,8) , (2,8) , (3,8).

3.2.6 Alpha Local Binary Pattern (alphaLBP)

Proposed by Kaplan et al. [22], the alpha LBP operator calculates the value of each pixel based on an angle value α . The code is the same of standard LBP, although the neighbors considered are on a line as shown in Figure 3.2.6 (a).

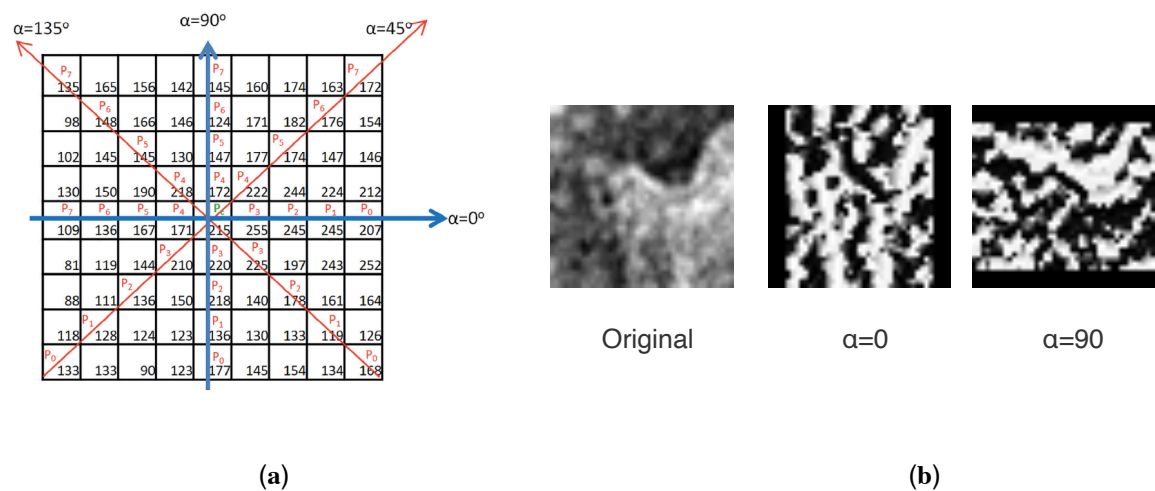


Figure 3.2.6. Kaplan et al. [22] proposed method. (a) Angle based neighbors. (b) Example of application on a TEM image of Influenza Virus with various angle.

This method has similar performance with standard LBP and the same pattern length but it is helpful to find image micro pattern. Like in LBP from resulted image (Figure 55 (b)) an histogram of pattern frequency is extracted. In this study we use a 8 neighbors line.

3.2.7 Heterogeneous Auto-Similarities of Characteristics (HASC)

HASC [26] combine linear relations by covariances (COV) and nonlinear associations with entropy combined with mutual information (EMI) of heterogeneous dense feature maps.

Covariance matrices are used as descriptors because they are low in dimensionality, robust to noise and, more important the covariance among two features describe the features of the joint PDF.

The entropy (E) of a random variable measures the uncertainty of its value, and the mutual information (MI) of two random variables captures their generic linear and nonlinear dependencies. HASC divides the image in portion, it calculate the EMI matrix and then concatenate the vectorized EMI and COV.

3.2.8 Local Concave Micro Structure Pattern (LCvMSP)

Differently from LBP, LCvMSP (Merabet et al. [28]) calculate the relation between center pixel and neighbors mathematically.

This method uses the median value of the 3x3 neighbors and the the entire image in both normal e grayscale value, this new two statistical triplets are used in LCvMSP.

Adding this two extra bit to Concave Binary Thresholding Function 1023 different pattern result, with improved statistical information (Alpasan et al. [29]).

3.2.9 JET Texton Learning

This method extract six Derivative of Gaussian (DtGs) for every pixel forming a six dimensions feature vector (jet vector), then k-means clustering is used to construct a jet texton dictionary (Roy et al. [30] for exhaustive information). The resulted is an histogram of the jet texton. Jet has excellent classification performance in large Dataset.

3.2.10 Adaptive Hybrid Patterns (AHP)

Introduced by Zhu et al. [37] it combines a Hybrid Texture Model (HTD) and Adaptive Quantization Algorithm (AQA). HTD is composed of local primitive features and global spatial structure and AQA improve noise robustness.

3.3 Texture descriptors Proposed from literature

A selection of descriptors from Santos et al. [24].

3.3.1 Local Ternary Pattern (LTP)

LTP (Tan & Triggs, [38]) is a simple LBP variant in which a threshold is set in the comparison, this help with different light condition in uniform area and provide better discrimination power, this allow a certain amount of noise before binarizing between the neighbor and the central pixel (Santos et al. [24]).

For every couple of pixel considered 3 values are possible (function $s(x)$), with 0 if the difference is minor of the threshold τ , with a resulting $3^{\text{number of neighbors}}$ histogram length. Santos decodes to divide the LBP+ e LBP- parts in two $2^{\text{number of neighbors}}$ histogram and then to concatenate them.

$$s(x) = \begin{cases} 1, & x \geq \tau \\ 0, & -\tau < x < \tau \\ -1, & \text{otherwise} \end{cases}$$

3.3.2 Local Phase Quantization (LPQ)

LPQ (proposed by Ojansivu [36]) use the Blur Invariance Property of the Fourier phase spectrum.

It considers a rectangular neighborhood where compute the 2-D Short Term Fourier Transform (STFT) to extract local phase information.

The nighbors rectangle in variable and results in a histogram of the pattern frequency equal to LBP.

3.3.3 Rotation Invariant Co-Occurrence Among Adjacent LBP

RI (Nosaka, Ohkawa, & Fukui, [39]) is a version of LBP that consider the spatial co-occurrence of the feature codes.

Each occurrence pair is labelled by the binary code and a spatial vector which connect the two centerpixels. Radius and neighbors are fixed as Santos et al. [24].

3.3.4 Local Binary Pattern Histogram Fourier

LHF (Ahonen et al. [41]) use the rotation of the LBP neighbors of a angle which is a multiple of $360/P$ where P is the number of neighbors.

The algorithm use the fact that if the image is rotated then the neighbors will be rotated by the same angle. Radius and neighbors are variable (Santos et al. [24]).

3.3.5 Dense LBP (DLBP)

DLBP (Ylioinas et al. [40]) use the same neighbors of LBP plus the corners between centered on the corner between center pixels.

It results in longer histogram to avoid noise. Radius and neighbors are variable (Santos et al. [24]).

3.3.6 Multi Quinary Coding (MQC)

Extending LTP function $s(x)$ with 2 threshold τ, θ there are 5 possible output:

$$s(x) = \begin{cases} 2, & x \geq \tau \\ 1, & \theta < x < \tau \\ 0, & 0 < x < \theta \\ -1, & -\theta < x < 0 \\ -2, & \text{otherwise} \end{cases}$$

Like LTP the labels are split into 4 binary patterns to reduce verbosity (Paci et al. [35]).

3.3.7 Edge (ED)

The idea behind the ED method is to focus on the important portions of an image and apply LBP like approach. In particular those salient regions are the edge and non-edge and we find them where the gradient function is higher. ED is used to create an ensemble of LBP like methods, for details read Santos et al. [24].

3.3.8 Difference of Gaussian (DoG)

DoG indicates the convolution of the original image with a 2D Dog filter obtained by the subtraction of two images blurred by different Gaussian Kernel with different variance, the result is similar to a band pass filter, for details read Santos et al. [24].

3.3.9 Bag of Feature (BoF)

BoF divides the images into regions and then extract different features from them, in order to build a visual vocabulary. From a new image feature vectors are extracted and assigned to the nearest matching terms from the vocabulary, for details read Santos et al. [24].

3.4 Deep Learning

Deep learning has revolutionized the field of machine learning. Deep learning can be implemented by means of several different algorithms, all of which are marked by a cascade of many processing layers organized in a hierarchical structure.

Each of these layers add a level of abstraction to the overall representation. In the image interpretation task, layers close to the input deal with low-level features like edges and texture.

These low-level features can be combined together to build a more complex representation. For example, at the second level, features like image patches and contours might be considered. Layer by layer, complexity increases.

The approach to deep learning considered in this paper is based on Convolutional Neural Networks (CNNs) (Krizhevsky et al. [31]).

Below, the deep learning-based approach considered in this work will be detailed. It should be pointed out that it is used as feature extraction method, where the last average pooling layer is considered as a feature vector and exploited in a fashion similar to how handcrafted features are commonly employed.

As neural network the DenseNet201 (Huang et al. [32]) has been used.

DenseNet is an evolution of ResNet which includes dense connections among layers: each layer is connected to each following layer in a feed-forward fashion.

Therefore the number of connections increases from the number of layers L to $L \times (L+1)/2$. DenseNet improves the performance of previous models at the cost of an augmented computation requirement. DenseNet accepts images of 224×224 pixels.

The training options are the following: 50 epochs for training, mini-batch of 30 observations, learning rate of 0.001, the training data are shuffled before each training epoch.

As data augmentation protocol we independently reflect the image in both the left-right (*RandXReflection*) and the top-bottom (*RandYReflection*) directions with 50% probability. We also linearly scale the image along both axes by two random numbers in [1, 2] (*RandXScale* and *RandYScale*).

4. Results

As already mentioned in the introduction, the dataset used can be found at the following link: http://www.cb.uu.se/_Gustaf/virustexture/ and is described by Kylberg et al. [2]. It contains 1500 41×41 Transmission Electron Microscopy (TEM) images of viruses belonging to 15 different species (specifically: Adenovirus, Astrovirus, CCHF, Cowpox, Dengue, Ebola, Influenza, Lassa, Marburg, Norovirus, Orf, Papilloma, Rift Valley, Rotavirus, Westnile). We see some examples in figure 2.7.

The virus dataset used in this paper is only one of two original datasets. The first dataset is referred to as the “object scale” dataset because the radius of the virus in each image is 20 pixels. The second dataset (not publicly available) is referred to as the “fixed scale” dataset because each virus image is represented by a direct scale where the size of 1 pixel corresponds to 1 nm; this dataset was not used in our tests because of copyright issues.

In the next [Table 4.1](#) we report performance of the texture descriptors here tested. Clearly the performance is very different considering different descriptors, to avoid any overfitting (i.e. to choose a set of feature extractor using a small training set) we have combined all the tested approaches.

JET	scLBP	AHP	HASC	Gradient+ARCS LBP	ARCSLB P	AlphaLBP	SigmaARC SLBP	DLBP	LCvMSP
58.93	69.47	76.60	68.40	61.00	79.93	64.13	75.40	70.33	64.67

Table 4.1. Performance of the set of texture descriptor here tested.

In [Table 4.2](#) we report the following ensemble:

- NewSet, sum rule among the methods reported in table 1, it is interesting to note that the fusion strongly outperforms the best stand-alone approach;
- OLD, it is previous set proposed in Santos et al. [4]
- HandC, it is the fusion by sum rule among the handcrafted methods of NewSet and OLD, this ensemble does not boost the performance of NewSet significantly.
- DeepL, it is the SVM trained using the last average pooling layer, notice that using DenseNet201 as classifier a lower 78.93% accuracy is obtained;
- HandC+DeepL is the sum rule between HandC and DeepL, before the fusion the scores of HandC and DeepL are normalized to mean 0 and standard deviation 1.

NewSet	OLD	HandC	DeepL	HandC+DeepL
85.40	85.67	86.13	86.40	89.47

Table 4.2. Performance of the ensemble.

Finally, in [Table 4.3](#) we compare our approach with other methods already reported in the literature using the same dataset with the same testing protocol.

Table 4.3. Comparison with the literature on the object scale dataset

Here	DenseNet	PCA	Fusion	LBPF	RDPF	RDPF +LBPF	MPMC	NewF
2020	[7] 2020	[9] 2018	[8] 2020	[2] 2011 fixed scale	[2] 2011	[2] 2011 fixed + object scale	[6] 2016	[24] 2015
89.47	89.00	88	87.27	79	78	87	86.2	85.7

In 2011 Kylberg et al. [\[2\]](#) the results in RDPF e RDPF + LBPF are obtained on the fixed scale version of our dataset that is not available online so a comparison is not possible. In the fixed version image 1 pixel corresponds to 1 nanometer, the virus in this study have a diameter from 25nm to 270nm, object scale image is always resized to 41x41 pixels.

Our ensemble obtains performance comparable with the best result already published.

5. Conclusions

In this paper, we have proposed an ensemble of handcrafted descriptors and deep learning features for the classification of transmission electron microscopy images of viruses.

For each descriptor a different SVM is trained, the set of SVMs is combined by sum rule, the proposed ensemble obtains state of the art performance in largely used dataset: clearly to combine handcrafted descriptors and deep learning features permits to boost the performance that can be obtained using only handcrafted descriptors or deep learning.

The set of handcrafted is mainly based on Local Binary Pattern variants, instead the deep learning approach is based on a DenseNet201 network, pretrained on ImageNet and then tuned in the virus dataset. The last average pooling layer of DenseNet201 is used as feature extractor for representing the images, these features are used to train a SVM classifier.

The MATLAB code of the proposed ensemble is available at <https://github.com/LorisNanni>.

Author Contributions: L.N. conceived of the presented idea., L.N., E.dL.,MF performed the experiments and wrote the manuscript

Funding: This research received no external funding.

Acknowledgments: The authors thank NVIDIA Corporation for supporting this work by donating a Titan Xp GPU. The authors would like to thank Dr. Gustaf Kylberg for sharing the virus dataset and his MATLAB code.

Conflicts of Interest: The authors declare no conflicts of interest.

References

1. Matuszewski, B.j., and L.-K. Shark. "Hierarchical Iterative Bayesian Approach to Automatic Recognition of Biological Viruses in Electron Microscope Images." Proceedings 2001 International Conference on Image Processing (Cat.No.01CH37205), doi:10.1109/icip.2001.958499.
2. Kylberg, Gustaf, et al. "Virus Texture Analysis Using Local Binary Patterns and Radial Density Profiles." Progress in Pattern Recognition, Image Analysis, Computer Vision, and Applications Lecture Notes in Computer Science, 2011, pp. 573–580., doi:10.1007/978-3-642-25085-9_68.
3. Proen  a, Maria C., et al. "Texture Indicators for Segmentation of Polyomavirus Particles in Transmission Electron Microscopy Images." Microscopy and Microanalysis, vol. 19, no. 5.
4. Santos, Florentino Luciano Caetano Dos, Nanni, Loris et al. "Computer Vision for Virus Image Classification." Biosystems Engineering, vol. 138, 2015, pp. 11–22., doi:10.1016/j.biosystemseng.2015.01.005.
5. Nanni, L. et al. "Virus image classification using different texture descriptors." (2014).
6. Wen, Zhijie, et al. "Virus Image Classification Using Multi-Scale Completed Local Binary Pattern Features Extracted from Filtered Images by Multi-Scale Principal Component Analysis." Pattern Recognition Letters, vol. 79, 2016, pp. 25–30., doi:10.1016/j.patrec.2016.04.022.
7. Geus, Andr   R. De, et al. "Variability Evaluation of CNNs Using Cross-Validation on Viruses Images." Proceedings of the 15th International Joint Conference on Computer Vision, Imaging and Computer Graphics Theory and Applications, 2020, doi:10.5220/0009352106260632.
8. Backes, Andre R., and Jarbas Joaci De Mesquita Sa Junior. "Virus Classification by Using a Fusion of Texture Analysis Methods." 2020 International Conference on Systems, Signals and Image Processing (IWSSIP), 2020, doi:10.1109/iwssip48289.2020.9145.
9. Wen, Zhi-Jie, et al. "Latent Local Feature Extraction for Low-Resolution Virus Image Classification." Journal of the Operations Research Society of China, vol. 8, no. 1, 2018, pp. 117–132., doi:10.1007/s40305-018-0212-8.
10. Virus Taxonomy: 2019 Release. International Committee on Taxonomy of Viruses.
11. Breitbart, Mya, and Forest Rohwer. "Here a Virus, There a Virus, Everywhere the Same Virus?" Trends in Microbiology, vol. 13, no. 6, 2005, pp. 278-284., doi:10.1016/j.tim.2005.04.003.
12. Insect-specific viruses and their potential impact on arbovirus transmission - Nikos Vasilakis, Robert Tesh, Current Opinion in Virology - 2015, doi:10.1038/ni0306-217
13. Pathogenesis: Of host and pathogen , Nature Immunology, 2006 doi:10.1038/ni0306-217.
14. Chinchar, V.gregory. "Replication Of Viruses." Encyclopedia of Virology, 1999, pp. 1471–1478., doi:10.1006/rwvi.1999.0245.
15. Auladell, Maria, et al. "Recalling the Future: Immunological Memory Toward Unpredictable Influenza Viruses." Frontiers in Immunology, vol. 10, 2019, doi:10.3389/fimmu.2019.01400.
16. Fauquet, C.m. "Taxonomy, Classification and Nomenclature of Viruses." Encyclopedia of Virology, 2008, pp. 9–23., doi:10.1016/b978-012374410-4.00509-4.
17. Hunter, Philip. "Viral Taxonomy." EMBO Reports, vol. 18, no. 10, 2017, pp. 1693–1696., doi:10.15252/embr.201744982.
18. Ojala, Timo, et al. "A Comparative Study of Texture Measures with Classification Based on Featured Distributions." Pattern Recognition, vol. 29, no. 1, 1996, pp. 51–59..
19. Kobayashi, Takumi. "Discriminative Local Binary Pattern for Image Feature Extraction." Computer Analysis of Images and Patterns Lecture Notes in Computer Science.
20. Ryu, Jongbin, et al. "Sorted Consecutive Local Binary Pattern for Texture Classification." IEEE Transactions on Image Processing, vol. 24, no. 7, 2015, pp. 2254–2265., doi:10.1109/tip.2015.2419081.
21. El merabet, Y., et al. "Attractive-and-Repulsive Center-Symmetric Local Binary Patterns for Texture Classification." Engineering Applications of Artificial Intelligence, vol. 78, 2019, pp. 158–172., doi:10.1016/j.engappai.2018.11.011.
22. Alpaslan, N., and Kazim Hanbay. "Multi-Resolution Intrinsic Texture Geometry-Based Local Binary Pattern for Texture Classification." IEEE Access, vol. 8, 2020, pp. 54415–54430., doi:10.1109/access.2020.2981720.
23. Kaplan, K., Kaplan, et al. "Brain Tumor Classification Using Modified Local Binary Patterns (LBP) Feature Extraction Methods." Medical Hypotheses, vol. 139, 2020, p. 109696., doi:10.1016/j.mehy.2020.109696.
24. Santos, F.L.C.D., et al. "Computer Vision for Virus Image Classification." Biosystems Engineering, vol. 138, 2015, pp. 11–22., doi:10.1016/j.biosystemseng.2015.01.005.
25. Nanni, L., Brahnam, S., Ghidoni, S., Maguolo, G., General Purpose (GenP) Bioimage Deep Ensemble Combining New Data Augmentation Techniques and Handcrafted Features.
26. Biagio, M.S., Heterogeneous auto-similarities of characteristics (hasc): Exploiting relational information for classification, in IEEE Computer Vision (ICCV13). 2013: Sydney, Australia. p. 809-816.

27. Nanni, L., et al. "Animal Sound Classification Using Dissimilarity Spaces." 2020, doi:10.20944/preprints202010.0526.v1.
28. Merabet, Y.E., Ruichek, Y., Local concave-and-convex micro-structure patterns for texture classification Pattern Recognition, vol. 76, pp. 303–322, Apr. 2018, doi: 10.1016/j.patcog.2017.11.005.
29. Alpasan, N., and Kazim Hanbay. "Multi-Scale Shape Index-Based Local Binary Patterns for Texture Classification." IEEE Signal Processing Letters, vol. 27, 2020, pp. 660–664., doi:10.1109/lsp.2020.2987474.
30. Roy, S.K., et al. "Unconstrained Texture Classification Using Efficient Jet Texton Learning." Applied Soft Computing, vol. 86, 2020, p. 105910., doi:10.1016/j.asoc.2019.105910.
31. Krizhevsky, A., Sutskever, I., Hinton, G.E., ImageNet Classification with Deep Convolutional Neural Networks, Adv. Neural Inf. Process. Syst. (2012) 1–9. doi:<http://dx.doi.org/10.1016/j.protcy.2014.09.007>
32. Huang, G., Liu, Z., Maaten, L.V.D., Weinberger, K.Q., Densely connected convolutional networks, in: Proc. - 30th IEEE Conf. Comput. Vis. Pattern Recognition, CVPR 2017, 2017. doi:10.1109/CVPR.2017.243.
33. Nanni, L., Intelligenza Artificiale per Ingegneria Informatica. 2019.
34. Jongbin, R., et al. "Sorted Consecutive Local Binary Pattern for Texture Classification." IEEE Transactions on Image Processing, vol. 24, no. 7, 2015, pp. 2254–2265., doi:10.1109/tip.2015.2419081.
35. Paci, M., Nanni, L., Lahti, A., Aalto-Setala, K., Hyttinen, J., & Severi, S. (2013). Non-binary coding for texture descriptors in Sub-cellular and stem cell image classification. Current Bioinformatics, 8(2), 208e219.
36. Ojansivu V., Heikkilä J. (2008) Blur Insensitive Texture Classification Using Local Phase Quantization. In: Elmoataz A., Lezoray O., Nouboud F., Mammass D. (eds) Image and Signal Processing. ICISP 2008. Lecture Notes in Computer Science, vol 5099. Springer, Berlin, Heidelberg. https://doi.org/10.1007/978-3-540-69905-7_27
37. Zhu, Ziqi, You, Xinge, Chen, C. L. Philip, Too, Dacheng, Ou, Weihua, Jiang, Xiubao, & Zoe, Jixin. (2015). An adaptive hybrid pattern for noise-robust texture analysis. *Pattern Recognition*, 48, 2592-2608
38. Tan, X., & Triggs, B. (2010). Enhanced local texture feature sets for face recognition under difficult lighting conditions. *Image Processing, IEEE Transactions On*, 19(6), 1635–1650.
39. Nosaka, R., Ohkawa, Y., & Fukui, K. (2012). Feature Extraction Based on Co-occurrence of Adjacent Local Binary Patterns. In *Proceedings of the 5th Pacific Rim Conference on Advances in Image and Video Technology - Volume Part II* (pp. 82–91). Berlin, Heidelberg: Springer-Verlag.
40. Ylioinas, J., Hadid, A., Guo, Y., & Pietikäinen, M. (2013). Efficient image appearance description using dense sampling based local binary patterns. In *Computer Vision – ACCV 2012 Lecture Notes in Computer Science* (Vol. 7726, pp. 375–388).
41. Ahonen, T., Matas, J., Chu, H., & Pietikäinen, M. (2009). Rotation Invariant Image Description with Local Binary Pattern Histogram Fourier Features, 61–70.